Journal of Power Sources 266 (2014) 296–303

Contents lists available at ScienceDirect

Journal of Power Sources

journal homepage: www.elsevier.com/locate/jpowsour

Development of flexible secondary alkaline battery with carbon nanotube enhanced electrodes

Zhiqian Wang, Somenath Mitra*

Department of Chemistry and Environmental Science, New Jersey Institute of Technology, 161 Warren St, Newark, NJ 07102, USA

HIGHLIGHTS

- Design and fabrication of flexible rechargeable alkaline battery are presented.
- Electrodes additives improved rechargeability.
- Carbon nanotubes were effective electrode additives.
- Electrode rechargeability in the flexible platform was similar to that of conventional batteries.

GRAPHICAL ABSTRACT

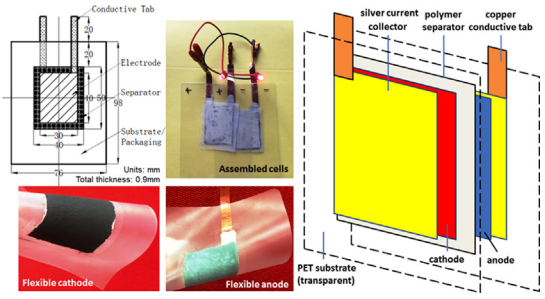

ARTICLE INFO

Article history:
Received 31 March 2014
Received in revised form
10 May 2014
Accepted 11 May 2014
Available online 20 May 2014

Keywords:
Flexible rechargeable alkaline battery
Carbon nanotube
Polyvinyl alcohol
Poly (acrylic acid)
Copolymer separator

ABSTRACT

We present the development of flexible secondary alkaline battery with rechargeability similar to that of conventional secondary alkaline batteries. Multiwalled carbon nanotubes (MWCNTs) were added to both electrodes to reduce internal resistance, and a cathode containing carbon black and purified MWCNTs was found to be most effective. A polyvinyl alcohol–poly (acrylic acid) copolymer separator served the dual functions of electrolyte storage and enhancing flexibility. Additives to the anode and cathode were effective in reducing capacity fades and improving rechargeability.

© 2014 Elsevier B.V. All rights reserved.

1. Introduction

The development of flexible electronics such as wearable equipment, displays, cell phones and smart cards requires flexible power sources such as batteries, supercapacitors and solar cells [1–7]. In general batteries have larger energy density than capacitors and are more commonly used for long-term energy storage. Different types of batteries, both primary and secondary ones are being developed to meet the requirement of flexible electronics where the trend is to decrease in size and increase in mobility [6–10]. Commercially available printing techniques including stencil and ink-jet printing can also be used for the production of such devices [11,12]. To date there have been significant efforts in the development of flexible batteries based on zinc–carbon and lithium-ion systems as well as those based on alternate chemistries [2,9,10]. Batteries have also been fabricated on textiles to serve as wearable electronics [13]. In many cases, secondary batteries which are more durable and eco-friendly are preferable to primary batteries. Lithium-ion batteries are the most widely studied among the flexible secondary batteries [9,10,14–18].

* Corresponding author. Tel.: +1 (973) 596 5611; fax: +1 (973) 596 3586.
E-mail address: somenath.mitra@njit.edu (S. Mitra).

http://dx.doi.org/10.1016/j.jpowsour.2014.05.029
0378-7753/© 2014 Elsevier B.V. All rights reserved.

The development of flexible batteries requires the use of novel materials that will provide optimum performance while retaining flexibility. Carbon nanotubes (CNTs), graphene and other nanocarbons have unique electrochemical and mechanical properties and are being explored as conductive additives in batteries electrodes, capacitors, current collectors and other active electrochemical materials [6,7]. Similar to carbon fibers, the CNTs can serve as the matrix or scaffolds for active materials [5,9,13,19]. Both single (SWCNTs) and multiwalled CNTs (MWCNTs) have been used in flexible batteries [6,7]. Another important component in such a battery is a flexible separator: paper, cellulose and polymers such as polyethylene oxide (PEO) and polyvinyl alcohol (PVA) membranes have been used reported [6,10,11,13].

Secondary alkaline batteries which use MnO_2 as active cathode material, Zn anode and alkaline electrolyte are an attractive alternative to lithium ion batteries [20–22]. Unlike the latter which have to be charged before the first use, the secondary alkaline batteries can be used out of the package. Similar to zinc–carbon cells, they are suitable for low drain and intermittent devices, and the costs of secondary alkaline batteries are relatively low. Known to work well for less deep discharges and frequent charges, secondary alkaline batteries are considered a good option in many applications including interfacing to solar cells [23–25]. Moreover, the secondary alkaline batteries are considered more eco-friendly than their lithium-ion counterparts where lithium is relatively toxic and organic electrolytes are used.

The development of flexible secondary alkaline batteries requires components including a separator to be stable at high pH while retaining flexibility. These are similar to their primary counterparts but require electrode additives to acquire rechargeability and a separator that is impermeable to zinc dendrites [26]. Flexible primary alkaline batteries have been reported in recent years [8,11,27], however flexible secondary alkaline batteries are yet to be reported. The objective of this study was to develop a flexible secondary alkaline battery and study its characteristics.

2. Experimental

The cathode paste was prepared by mixing electrolytic manganese dioxide powder (EMD, TRONOX, ≥92%, AB Grade), polyethylene oxide (PEO, Sigma Aldrich, Mv ~ 400,000) binder, magnesium oxide (Sigma Aldrich, 99.99%) and conductive additives. The conductive additives included synthetic graphite (Sigma Aldrich, <20 micron), multiwalled carbon nanotubes (MWCNTs, purity 95%, diameter 20–30 nm, length 10–30 μm, Cheap Tubes Inc. Brattleboro, VT, USA), and carbon black (Sigma Aldrich, <500 nm). All chemicals were used as received, except that some of the MWCNTs were purified or functionalized prior to the electrode preparation.

The purification and functionalization of CNTs were performed in a Microwave Accelerated Reaction System (Mode: CEM Mars) using experimental procedures previously reported by our laboratory [28]. After mixing the components in DI water, the paste was sonicated for at least 30 min using an ultrasonic homogenizer (Omni Sonic Ruptor 250) and then stirred for 20 h to form homogenous slurry. The dry cathode contained 2.0% by weight of MgO, 10% PEO, and the rest was EMD and conductive additives. The EMD to conductive additive ratios in the cathode mixture were varied and optimized.

The anode paste was prepared with zinc powder (Sigma Aldrich, ≤10 μm, ≥98%), PEO binder, zinc oxide powder (Sigma Aldrich, ≥99%), methyl cellulose (Sigma Aldrich, Mn ~ 40,000), Bismuth (III) oxide (Sigma Aldrich, 90–210 nm particle size, ≥99.8%) inhibitors, and conductive additives. The powders were mixed in the presence of DI water and then stirred to form a homogeneous anode paste. A typical dry anode contained 1% methyl cellulose, 5% PEO and 2% Bismuth (III) oxide. The amount of zinc, zinc oxide, conductive additives were subject to optimization.

A PVA (Mowiol 18-88, Sigma Aldrich, Mv ~ 130,000)–PAA (Sigma Aldrich, Mv ~ 450,000) copolymer separator was fabricated using the method described before [27]. The separator was soaked in the electrolyte for 2 h and cut into right sizes before use. A typical separator after soaking and cutting was 5 cm × 4 cm in size.

Swagelok-type cells using graphite rod current collectors were assembled to optimize the electrode formulation. For anode optimization, the cathode was fixed as 80% EMD, 2% MgO, 8% MWCNTs, and 10% PEO. Typical anode contained 2% Bi_2O_3, 5% PEO and 1% methyl cellulose unless otherwise specified. The amounts of carbons, Zn and ZnO were varied. For cathode optimization, the anode contained 72% Zn, 18% ZnO, 5% PEO, 2% MWCNTs, 1% methyl cellulose, 2% Bi_2O_3; cathode contained 2% MgO and 10% PEO while the amount of carbons and EMD were varied. The typical weights of the cathode and anode after drying were 0.03 g and 0.05 g respectively. The electrolyte was 9 M KOH solution with 6% ZnO.

Flexible electrodes were prepared by casting the electrode slurry onto the silver ink current collectors. The current collectors were prepared by manually applying silver ink (CircuitWriter, CAIG Laboratories. Inc.) to the adhesive side of polyethylene

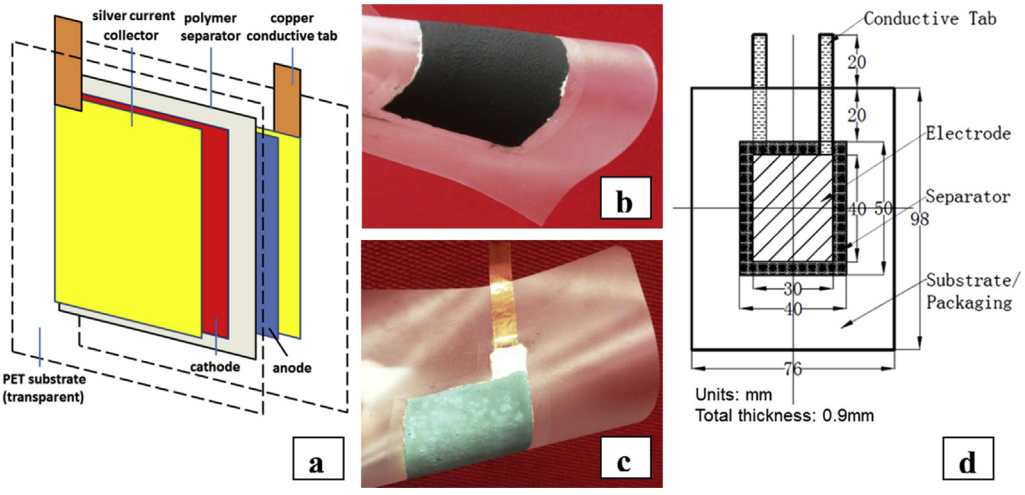

Fig. 1. (a) Structure of a flexible secondary alkaline battery; (b) photograph of flexible cathode, (c) flexible anode, (d) typical size of a flexible cell.

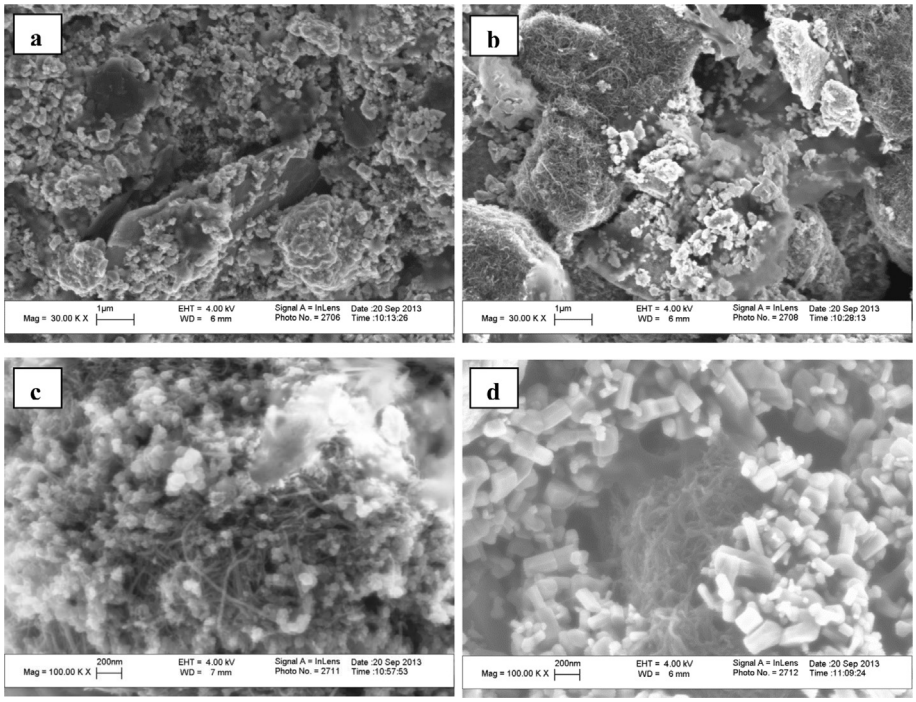

Fig. 2. SEM images of (a) cathode with graphite and carbon black; (b) cathode with MWCNTs; (c) cathode with carbon black and MWCNTs; (d) MWCNTs in anode.

terephthalate (PET) film coated with ethylene vinyl acetate copolymer (EVA) resin (CRC52005, 3 mil, Fellowes) to form a layer with silver loading of 3.6 mg cm^{-2}. The typical electrode area was 4 cm × 3 cm. Copper tapes (EMI Copper Foil Shielding Tape 1181, 6.35 mm, 3M™) were stuck to the current collector to serve as electrode tabs. After applying the slurry onto the current collector, the electrodes were allowed to dry at ~50 °C for 30 min. The last 5 min of drying was processed under vacuum (9.893 kPa). The drying was complete with no residual water. The typical weights of the cathode and anode after drying were 0.06 g and 0.125 g respectively. The battery was thermally sealed. Structure of the battery and flexible electrodes after drying has been shown in Fig. 1. In all the cells tested, zinc was in stoichiometric excess and there was enough to maintain the required anode conductivity, so in the electrochemical process MnO_2 was considered to be the limiting reagent.

Scanning electron microscope (SEM) images were collected on a LEO 1530 VP Scanning Electron Microscope. The electrochemical performances of the cells were measured by discharging and charging under constant current modes using a MTI Battery Analyzer (Richmond, CA). The fixed Swagelok-type cells were discharges at 1.48 mA to 0.9 V and overcharged at 2.96 mA to 2 V; while the flexible ones were discharged and charged at 4 and 8 mA respectively. The flexible batteries were also firmly attached over solid substrates of different shapes like and tested to examine electrochemical performance under bending conditions.

3. Results and discussion

The structure of a flexible battery is shown in Fig. 1. The flexible separator which is electrically nonconductive but has high ionic conductivity is placed between the electrodes and the whole assembly needs to demonstrate flexibility. Previously we have reported the development of a copolymer film made from PVA and PAA [27]. The copolymer film served as a separator as well as a medium for electrolyte storage, and it maintained its stability and flexibility. It is believed that this film could also be a promising candidate for the secondary cells.

3.1. Flexible cathode

Fig. 2 a–c shows scanning electron microscopy (SEM) images of cathodes formulated with different nanocarbons. Table 1 shows the energy-dispersive X-ray spectroscopy (EDX) data of different carbon nanotubes used to make cathodes. Acid functionalization introduced more oxygen into the CNTs in the form of COOH groups. The purification in dilute acids was not harsh and generated few defects [29]. These conductive additives were added into cathode to reduce the internal resistance.

The constant current discharge–charge curve of an alkaline cell is shown in Fig. 3. This typical cell contained 6% MWCNTs and 2% carbon black as conductive additives in the cathode, the anode contained zinc, zinc oxide as well as 2% MWCNTs, and the copolymer separator was placed between them. The upper/red (in the web version) curve shows the charge–discharge voltage patterns as a function of time, while the lower/blue curve shows the delivered capacity of each cycle in mAh. A cell was discharged to 0.9 V and recharged to 2 V to form a single cycle. The discharge pattern of the single cycle was similar to what has been reported before for primary cells [26].

Performances of different cells with different carbon forms are shown in Fig. 4, with theoretical capacity in Table 2. It shows delivered cell capacity during each discharge as a function of cycle number. Graphite which has been extensively used together with

Table 1
EDX data of different MWCNTs.

CNTs	C weight %	O weight %	Fe weight %	Ni weight %
CNT-raw	96.57	1.34	0.19	1.90
CNT-purified	97.66	0.82	–	1.52
CNT–COOH	86.81	13.19	–	–

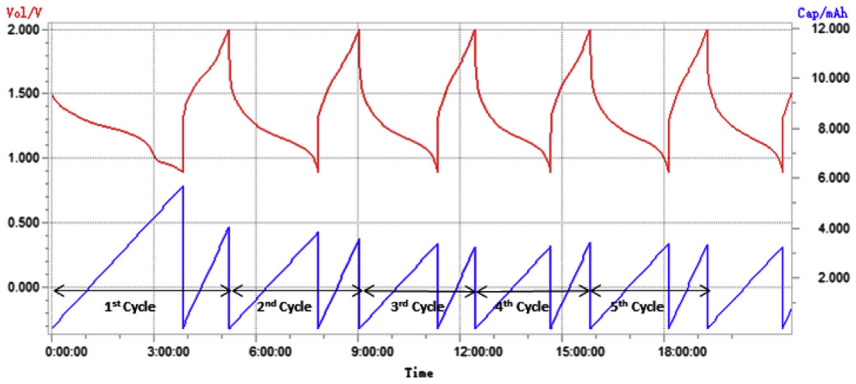

Fig. 3. Discharge and charge curve of a secondary alkaline cell.

carbon black in rechargeable alkaline batteries showed lower performance than the MWCNTs. The replacement of graphite by MWCNTs improved the cell performance. The purification of CNTs removed impurities which might have hindered the electrochemical reactions and therefore enhanced cell performance even further.

The functionalized CNTs showed lower performance due to the defects that lead to lower conductivity. Even in the first discharge, cells with functionalized CNTs showed lower capacity which was in line with what has been reported before [7,27]. This was different from lithium-ion batteries where higher levels of defects were known to enhance capacity [30,31]. Rechargeability was also compromised by the surface defects and higher resistance due to functionalization. The poor conductivity made electron transfer from Mn (III) particles more difficult during the charging cycle. The interaction between the alkaline electrolyte and the carboxylic groups on the CNTs may have also contributed to the degradation in performance. The electrolyte may have been partially neutralized causing a drop in surface concentration of OH^-, which reacted with Mn_2O_3 during the charging. The negative charge of COO^- groups might also repel the OH^-.

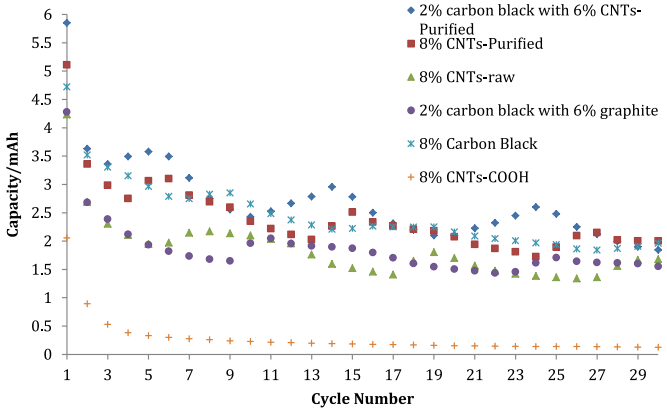

Fig. 4. Capacity as a function of cycle numbers for cells with different carbons.

We have reported in our previous publication [27] that the flexible battery electrodes tend to become fragile at high concentration of conductive additives thus decreasing the discharge performance. As a conductive additive carbon black showed good performance, however the electrodes were found to be more fragile than their MWCNT counterparts. Our results indicated that cathode with 6% purified MWCNTs and 2% carbon black showed optimum performance and flexibility (Fig. 5 and Table 3). CNTs and carbon black were more effective as conductive additives than graphite due to their better dispersibility. CNTs were dispersed together with carbon black in the cathode. The latter filled the small gaps and connected to conductive networks formed by CNTs. The unique shape of CNTs maintained the integrity of the electrodes during bending and imparted good mechanical properties. In another set of tests, when carbon black alone was used as the conductive additive, the electrode was more fragile and less effective under bending conditions. The CNTs and the carbon black also appeared to disperse well with MnO_2 and the long CNTs helped bridge the carbon black particles and formed better conductive networks. Electrode with 8% purified MWCNTs and 2% carbon black showed similar performance but capacity faded faster while the electrode flexibility was lower. Compared to primary cells reported before [27], the active material utilization was lower in the rechargeable batteries even in the first discharge, which could be partially attributed to the much higher amounts of non-conductive agents added to the electrode. For a cell with optimized formulation (consider electrode performance and flexibility), the first discharge showed approximately 79% utilization (243 mAh g^{-1}) of limiting active material manganese dioxide. This dropped to 38% (117 mAh g^{-1}) after the first 10 cycles, and after 30 cycles the manganese dioxide specific capacity dropped to approximately 105 mAh g^{-1}, which was 34% of the theoretical value of 308 mAh g^{-1} MnO_2. These values were similar to those reported for

Table 2
Theoretical/actual capacity of cells with different carbons in cathode.

Cells	Theoretical capacity (mAh)	Delivered capacity 1st cycle (mAh)	Delivered capacity 25th cycle (mAh)	Specific capacity of MnO_2 (mAh g^{-1}) 25th cycle
2% carbon black + 6% CNT-purified	6.8	5.85	2.478	112.2
8% CNT-purified	6.8	5.111	1.891	85.7
8% CNT-raw	6.8	4.235	1.36	61.6
2% carbon black + 6% graphite	6.8	4.279	1.708	77.4
8% carbon black	6.8	4.721	1.937	87.7
8% CNT–COOH	6.8	2.055	0.128	5.8

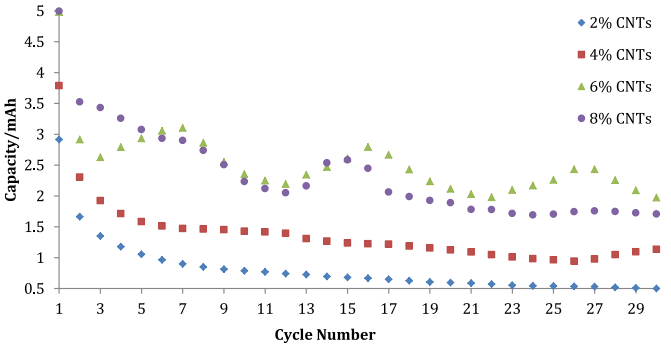

Fig. 5. Cycling of cells with cathodes containing different amount of purified CNTs and 2% carbon black.

Table 3
Theoretical/actual capacity of cells with purified CNTs in cathode.

Cells	Theoretical capacity (mAh)	Delivered capacity 1st cycle (mAh)	Delivered capacity 25th cycle (mAh)	Specific capacity of MnO_2 (mAh g^{-1}) 25th cycle
2% CNTs	7.31	2.915	0.538	22.7
4% CNTs	7.14	3.787	0.962	41.5
6% CNTs	6.8	4.982	2.26	102.4
8% CNTs	6.63	4.994	1.7	79

conventional (nonflexible) secondary alkaline cell electrodes (200–225 mAh g^{-1} during the first discharge; 75–125 mAh g^{-1} after 25 cycles [32]; and even lower elsewhere [22]).

3.2. Flexible anode

The MWCNTs dispersed well with the micron-sized zinc and bridged the conductive particles (Fig. 2d). Zinc was oxidized to zinc oxide during discharge. Other composites such as polyethylene oxide (PEO), methyl cellulose and Bi_2O_3 were non-conductive. In order to maintain the anode conductivity, MWCNTs were added into the anode. Three different CNTs were tested (Fig. 6 and Table 4). Unlike the cathode, the purification of CNTs appeared to provide little improvement. However, the residual metal catalysts in the CNT preparation might have caused secondary reactions or self-discharge and therefore the purification of CNTs was still important. CNT–COOH showed better performance during the first 10 cycles; however the capacity faded faster. It is concluded that during the beginning cycles with sufficient zinc and electrolyte, the lower conductivity of CNT–COOH was compromised by the higher conductivity of zinc. During the following cycles when zinc was consumed or coated with zinc oxide, the electrode conductivity

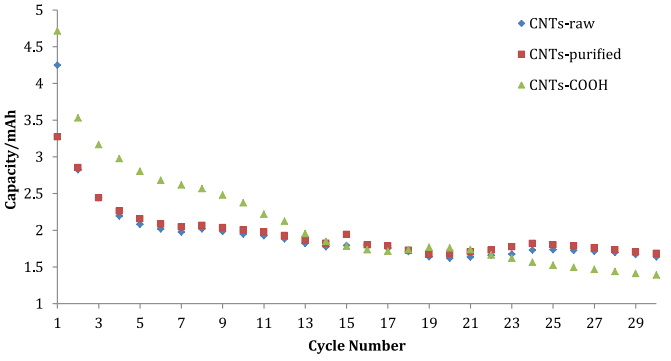

Fig. 6. Effects of cycling in cells with different types of CNTs (2% by weight) in anode.

Table 4
Theoretical/actual capacity of cells with different CNTs (2%) in anode.

Cells	Theoretical capacity (mAh)	Delivered capacity 1st cycle (mAh)	Delivered capacity 25th cycle (mAh)	Specific capacity of MnO_2 (mAh g^{-1}) 25th cycle
2% CNTs-raw	6.8	4.247	1.735	78.6
2% CNTs–COOH	6.8	4.715	1.524	69
2% CNTs-purified	6.8	3.273	1.802	81.5

decreased and CNT–COOH was not as good a conductive additive as the other CNTs.

An increase in the amount of CNTs added to the anode compromised electrode flexibility just like it did in the cathode. A concentration of 2% MWCNTs in the anode was a balance between optimum performance and flexibility (Fig. 7 and Table 5). Without CNTs, the cell capacity faded rather quickly. The CNTs also led to optimum viscosity which allowed easier casting, helped prevent the formation of an impervious Zn/ZnO layer, and kept channels open for electrolyte diffusion.

Different Zn to ZnO ratios were also used to optimize the anode formulation. The performance of cells with different Zn/ZnO ratio is shown in Fig. 8 and Table 6. ZnO was critical to inhibiting gassing. While it could be reduced back to zinc during charging; it could also reduce the available amount of electrolyte. ZnO is known to react with OH^- to form zincates which is a common occurrence in all alkaline cells [32,33]. Cells with a Zn to ZnO ratio of 5:1 showed the best rechargeability, which was followed closely by a 4:1 ratio. Cells with higher amount of ZnO showed lower performance due to the low conductivity of ZnO while those with very low ZnO concentration showed poor rechargeability. It is evident that the relatively higher concentration of ZnO in the anode was an important feature of the secondary alkaline cell and was critical for rechargeability.

3.3. Effect of charge–discharge cycles

The capacity is known to fade with discharge–charge cycles in conventional secondary alkaline cells. There are different reports

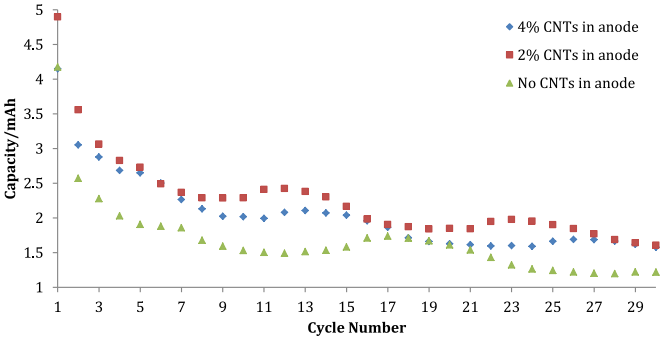

Fig. 7. Effects of cycling in cells with different amounts of purified CNTs in anode.

Table 5
Theoretical/actual capacity of cells with purified CNTs in anode.

Cells	Theoretical capacity (mAh)	Delivered capacity 1st cycle (mAh)	Delivered capacity 25th cycle (mAh)	Specific capacity of MnO_2 (mAh g^{-1}) 25th cycle
0% CNTs	6.8	4.177	1.243	56.3
2% CNTs	6.8	4.897	1.901	86.4
4% CNTs	6.8	4.151	1.662	75.3

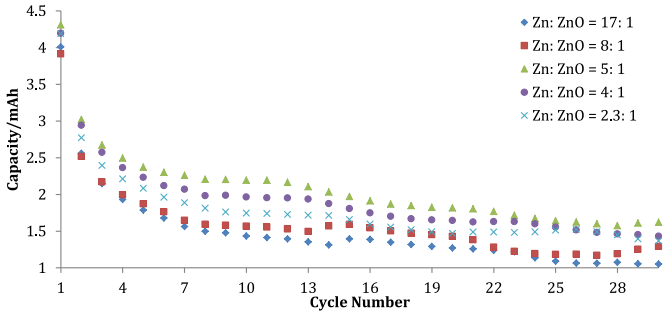

Fig. 8. Effects of cycling in cells with different Zn to ZnO ratio in anode (all contained 2% purified CNTs).

Table 6
Theoretical/actual capacity of cells with different Zn to ZnO ratio.

Zn:ZnO ratio of cells	Theoretical capacity (mAh)	Delivered capacity 1st cycle (mAh)	Delivered capacity 25th cycle (mAh)	Specific capacity of MnO_2 (mAh g^{-1}) 25th cycle
17:1	6.8	4.01	1.09	49.37
8:1	6.8	3.912	1.182	53.54
5:1	6.8	4.31	1.642	74.37
4:1	6.8	4.195	1.555	70.43
2.3:1	6.8	4.188	1.514	68.58

on the mechanisms behind the decrease in capacity with increased cycling. It has been known that soluble zincates enter into MnO_2 lattice and alter the shape of the anode [20,21]. Hence MgO was added to the cathode to block the incorporation of zincate ions into the MnO_2 region [34], while methyl cellulose was added into anode as gelling agent to prevent the alteration of anode morphology [21]. These were particularly important for reducing capacity fades and ensuring better rechargeability. The degradation of anode materials with cycling is an important issue for all rechargeable batteries. Fig. 1c shows the original anode while Fig. 9a shows anode materials after 30 cycles.

Parts of the anode formed hard shell with darker color which is in line with what has been reported elsewhere [21]. The SEM images of the light and dark parts of the anode are shown in Fig. 9. The hardened dark parts appeared to be less porous. It is believed that the dark layer is composed of Zn deposits which were formed by the reduction of precipitated ZnO, and such layers are less permeable to electrolytes and hinder further electrochemical reactions [35–37]. The reduction of this shell is possible with the addition of gelling agents such as methyl cellulose [21]. As shown in Fig. 10 and Table 7, the cell performance improved with the addition of optimum amount of methyl cellulose. However addition of very high concentrations of gelling agent made the anode fragile and compromised flexibility. The performance after optimization was in line with what has been reported for conventional batteries [21].

The separator was an important component of the flexible battery. Cells with traditional glass fiber separator failed but this problem was overcome by using copolymer separator that has been described before and is not discussed for brevity (Fig. 10).

3.4. Performance of flexible cells

The cells had an open circuit voltage of 1.5 V. Two cells were connected in series to power LED lights as shown in Fig. 11. The performance of the flexible cell under bending conditions is shown in Fig. 12. Cells were bent in different ways: they were bent in 90°, folded in half (180°), and rolled into cylinders with a relatively narrow radius of 2 cm. The copolymer separator was effective in the secondary alkaline cell. The flexible cells remained functional under bending and folding conditions; however the performance were compromised (theoretical capacity was 13.5 mAh). During bending, parts of the electrodes and separator stacked together and enhanced contact in some sections while other parts separated to lose contact. This caused fluctuation/drop in cell performance. Another reason was that the packaging techniques allowed relatively lower amount of electrolyte to be incorporated in the cells. Performance could be further improved by improving the internal contacts and electrolyte storage with more advanced packaging methods. The cell performance could also be improved by using MnO_2 nanoparticles [38,39].

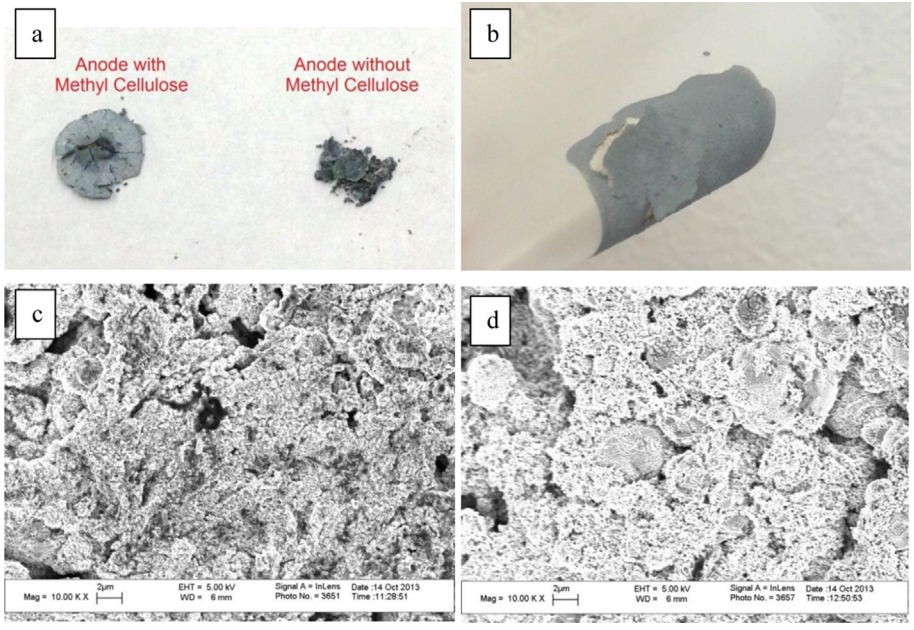

Fig. 9. (a) Anode material after 30 cycles; (b) anode material with higher amount of gelling agent; (c) SEM image of lighter part of anode; (d) SEM image of darker part of anode.

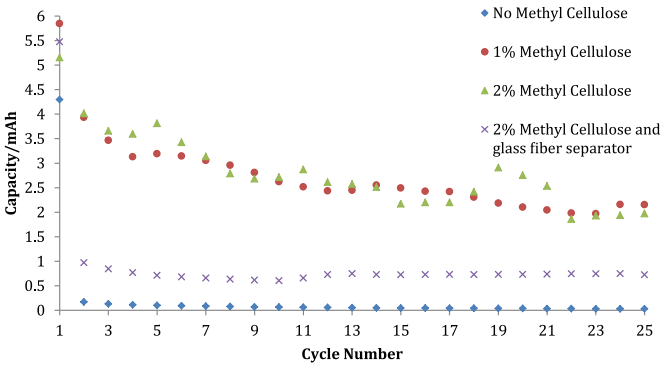

Fig. 10. Cycling of cells with different amounts of methyl cellulose in anode and glass fiber separator.

Table 7
Theoretical/actual capacity of cells with/without methyl cellulose in anode.

Cells	Theoretical capacity (mAh)	Delivered capacity 1st cycle (mAh)	Delivered capacity 25th cycle (mAh)	Specific capacity of MnO_2 (mAh g^{-1}) 25th cycle
0% methyl cellulose	6.8	4.296	Fail	Fail
1% methyl cellulose	6.8	5.848	2.154	97.6
2% methyl cellulose	6.8	5.155	1.975	89.5
2% methyl cellulose with glass fiber separator	6.8	5.474	0.723	32.7

4. Conclusions

In summary, flexible secondary alkaline batteries were fabricated successfully. Once optimized, they showed enhancement in both electrode performance and flexibility. Purified multiwalled carbon nanotubes were found to be effective conductive cathode additives in combination with carbon black. The addition of small amounts of carbon nanotubes also helped anode performance by reducing electrode resistance when the concentration of ZnO was relatively high. The addition of methyl cellulose to the electrodes enhanced rechargeability by providing pathways for electrolyte mobility.

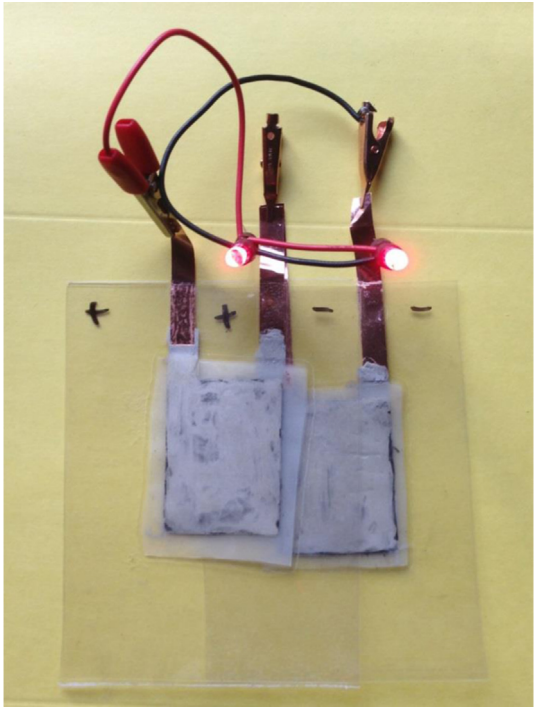

Fig. 11. Flexible secondary alkaline batteries powering up LED lights.

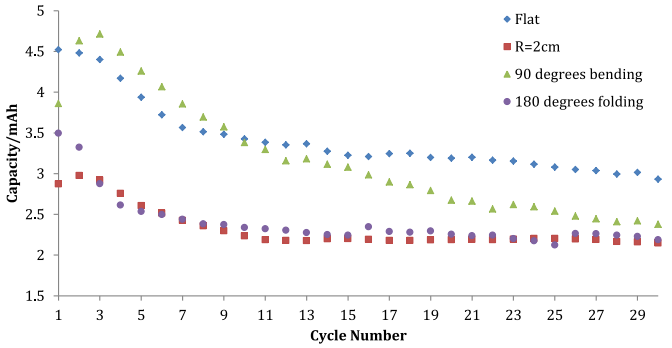

Fig. 12. Effects of cycling under different bending conditions.

Acknowledgments

The carbon nanotube processing part of the work was partially funded by the National Institute of Environmental Health Sciences (NIEHS) under Grant Number RC2 ES018810. Any opinions, findings, and conclusions or recommendations expressed in this material are those of the author(s) and do not necessarily reflect the views of the NIEHS.

References

[1] J.P. Coleman, A.T. Lynch, P. Madhukar, J.H. Wagenknecht, Sol. Energy Mater. Sol. C 56 (1999) 395–418.
[2] R. Hahn, H. Reichl, in: Digest of Papers. The Third International Symposium on Wearable Computers, 1999, 1999, pp. 168–169.
[3] L. Bao, J. Zang, X. Li, Nano Lett. 11 (2011) 1215–1220.
[4] A.C. Siegel, S.T. Phillips, M.D. Dickey, N. Lu, Z. Suo, G.M. Whitesides, Adv. Funct. Mater. 20 (2010) 28–35.
[5] K. Gao, Z. Shao, J. Li, X. Wang, X. Peng, W. Wang, F. Wang, J. Mater. Chem. A 1 (2013) 63–67.
[6] P. Hiralal, S. Imaizumi, H.E. Unalan, H. Matsumoto, M. Minagawa, M. Rouvala, A. Tanioka, G.A.J. Amaratunga, ACS Nano 4 (2010) 2730–2734.
[7] Z. Wang, N. Bramnik, S. Roy, G. Di Benedetto, J.L. Zunino Iii, S. Mitra, J. Power Sources 237 (2013) 210–214.
[8] A.M. Gaikwad, G.L. Whiting, D.A. Steingart, A.C. Arias, Adv. Mater. 23 (2011) 3251–3255.
[9] X. Jia, C. Yan, Z. Chen, R. Wang, Q. Zhang, L. Guo, F. Wei, Y. Lu, Chem. Commun. 47 (2011) 9669–9671.
[10] L. Hu, H. Wu, F. La Mantia, Y. Yang, Y. Cui, ACS Nano 4 (2010) 5843–5848.
[11] A.M. Gaikwad, D.A. Steingart, T. Nga Ng, D.E. Schwartz, G.L. Whiting, Appl. Phys. Lett. 102 (2013).
[12] Y. Zhao, Q. Zhou, L. Liu, J. Xu, M. Yan, Z. Jiang, Electrochim. Acta 51 (2006) 2639–2645.
[13] L. Bao, X. Li, Adv. Mater. 24 (2012) 3246–3252.
[14] N.A. Hamid, S. Wennig, S. Hardt, A. Heinzel, C. Schulz, H. Wiggers, J. Power Sources 216 (2012) 76–83.
[15] J.F. Ihlefeld, P.G. Clem, B.L. Doyle, P.G. Kotula, K.R. Fenton, C.A. Apblett, Adv. Mater. 23 (2011) 5663–5667.
[16] L. Noerochim, J.-Z. Wang, S.-L. Chou, D. Wexler, H.-K. Liu, Carbon 50 (2012) 1289–1297.
[17] H.M. Ren, Y.H. Ding, F.H. Chang, X. He, J.Q. Feng, C.F. Wang, Y. Jiang, P. Zhang, Appl. Surf. Sci. 263 (2012) 54–57.
[18] J. Saunier, F. Alloin, J.Y. Sanchez, G. Caillon, J. Power Sources 119–121 (2003) 454–459.
[19] R.K. Sharma, L. Zhai, Electrochim. Acta 54 (2009) 7148–7155.
[20] F. Beck, P. Rüetschi, Electrochim. Acta 45 (2000) 2467–2482.
[21] Y. Shen, K. Kordesch, J. Power Sources 87 (2000) 162–166.
[22] M. Ghaemi, R. Amrollahi, F. Ataherian, M.Z. Kassaee, J. Power Sources 117 (2003) 233–241.
[23] X.C. Lau, C. Desai, S. Mitra, Sol. Energy 91 (2013) 204–211.
[24] G. Dennler, S. Bereznev, D. Fichou, K. Holl, D. Ilic, R. Koeppe, M. Krebs, A. Labouret, C. Lungenschmied, A. Marchenko, D. Meissner, E. Mellikov,

J. Méot, A. Meyer, T. Meyer, H. Neugebauer, A. Öpik, N.S. Sariciftci, S. Taillemite, T. Wöhrle, Sol. Energy 81 (2007) 947–957.
[25] X.C. Lau, Z. Wang, S. Mitra, Appl. Phys. Lett. 103 (2013) 243108.
[26] P. Arora, Z. Zhang, Chem. Rev. 104 (2004) 4419–4462.
[27] Z. Wang, Z. Wu, N. Bramnik, S. Mitra, Adv. Mater. 26 (2014) 970–976.
[28] Y. Chen, S. Mitra, J. Nanosci. Nanotechnol. 8 (2008) 5770–5775.
[29] Y. Chen, Z. Iqbal, S. Mitra, Adv. Funct. Mater. 17 (2007) 3946–3951.
[30] B.J. Landi, M.J. Ganter, C.D. Cress, R.A. DiLeo, R.P. Raffaelle, Energy Environ. Sci. 2 (2009) 638–654.
[31] S.L. Candelaria, Y. Shao, W. Zhou, X. Li, J. Xiao, J.-G. Zhang, Y. Wang, J. Liu, J. Li, G. Cao, Nano Energy 1 (2012) 195–220.
[32] A. Stani, W. Taucher-Mautner, K. Kordesch, J. Daniel-Ivad, J. Power Sources 153 (2006) 405–412.
[33] R. Shivkumar, G. Paruthimal Kalaignan, T. Vasudevan, J. Power Sources 55 (1995) 53–62.
[34] M. Minakshi, M. Blackford, M. Ionescu, J. Alloys Compd. 509 (2011) 5974–5980.
[35] C. Cachet, Z. Chami, R. Wiart, Electrochim. Acta 32 (1987) 465–474.
[36] C. Cachet, B. Saïdani, R. Wiart, Electrochim. Acta 33 (1988) 405–416.
[37] C. Cachet, B. Saïdani, R. Wiart, Electrochim. Acta 34 (1989) 1249–1250.
[38] J. Zang, X. Li, J. Mater. Chem. 21 (2011) 10965–10969.
[39] F.Y. Cheng, J. Chen, X.L. Gou, P.W. Shen, Adv. Mater. 17 (2005) 2753–2756.